Desalination and Water Treatment
www.deswater.com
doi: 10.1080/19443994.2014.924031

55 (2015) 1220–1228
July

Taylor & Francis
Taylor & Francis Group

Zinc hexacyanoferrate loaded mesoporous MCM-41 as a new adsorbent for cesium: equilibrium, kinetic and thermodynamic studies

Somayeh Vashnia[a], Hamed Tavakoli[b], Ramin Cheraghali[a], Hamid Sepehrian[c,*]

[a]*Chemistry Department, Saveh Branch, Islamic Azad University, Saveh, Iran, Tel. +98 9127151843; email: somayeh.vashnia@yahoo.com (S. Vashnia), Tel. +98 9122936072; email: ramin.cheraghali@yahoo.com (R. Cheraghali)*
[b]*Faculty of Science, Nour Branch, Islamic Azad University, Nour, Iran, Tel. +98 9112220577; email: ha.tavakoli@gmail.com*
[c]*Nuclear Science and Technology Research Institute, P.O. Box 11365/8486, Tehran, Iran, Tel. +98 2188221117; Fax: +98 2188221116; email: hsepehrian@aeoi.org.ir*

Received 6 October 2013; Accepted 8 May 2014

ABSTRACT

Mesoporous MCM-41 has been modified by loading of zinc hexacyanoferrate (ZnHCF) as a new adsorbent for cesium. The ZnHCF-loaded mesoporous MCM-41 (ZnHCF-MCM-41) was characterized using powder X-ray diffraction and nitrogen adsorption–desorption isotherm data, fourier transform infrared spectroscopy, scanning electron microscopy coupled with energy dispersive X-ray. The cesium removal performance of ZnHCF-MCM-41 from aqueous solutions has been studied, and the effect of the various parameters, such as initial pH value of solution, contact time, temperature, and initial concentration of the cesium ion on the adsorption efficiencies of ZnHCF-MCM-41 were investigated systematically by batch experiments. Adsorption kinetics was better described by the pseudo-second-order model and thermodynamic parameters indicated the adsorption process was feasible, endothermic, and spontaneous in nature. Adsorption isotherm of ZnHCF-MCM-41 was studied and the fitted results indicated that Langmuir model could well represent the adsorption process. The maximum adsorption capacity of Cs^+ onto ZnHCF-MCM-41 was found to be 103.09 mg g^{-1}.

Keywords: Mesoporous MCM-41; Modification; Zinc hexacyanoferrate; Cesium sorption

1. Introduction

Among the used inorganic ion exchanger materials for the removal of ^{137}Cs from nuclear waste streams, the metal hexacyanoferrates (MHCFs) have a profound position due to their high selectivity and ion exchange capacity for Cs-isotopes. On the other hand, insoluble MHCFs had gelatinous form or small particle size and might even be colloidal, so in this form were unsuitable for practical applications [1].

For solving this problem, several researchers have reported the use of an inert solid supports such as porous silica for CuHCF [1] and NiHCF [2], polyacrylonitrile binding polymer for CuHCF and NiHCF [3], zeolites for NiHCF [4,5], vermiculite for CuHCF [6], activated carbon for CuHCF [7], and mesoporous ceramic backbone for CuHCF [8].

MCM-41 is one of the important inorganic adsorbents, which possess unique features such as large uniform pore sizes (1.5–10 nm), highly ordered nanochannels and large surface areas (~1,500 $m^2 g^{-1}$), and large pore volume with regular hexagonal structure

*Corresponding author.

[9,10]. These characteristics render MCM-41 as an ideal support for the loading of MHCFs.

In this study, a new adsorbent was synthesized by loading of zinc hexacyanoferrate (ZnHCF) onto mesoporous MCM-41 as a support, and its adsorption behavior for cesium ions was investigated. The adsorption kinetics, adsorption thermodynamic, adsorption isotherm, and pH effect on cesium sorption were also studied in detail.

2. Experimental

2.1. Reagents

All the chemicals used were of analytical grade from Merck (Darmstadt, Germany), expect cethyltrimethylammonium bromide (CTAB) which was supplied by Aldrich (Milwaukee, WI, USA).

2.2. Preparation of the mesoporous MCM-41

MCM-41 was prepared according to our previously published papers [11,12]. In a typical procedure, 0.6 g of CTAB was dissolved in 23 g of demineralized water and stirred for 15 min with the rate of 140 rpm, and then 3 g of sodium silicate was added to it and was further stirred for 30 min. The pH of the mixture was adjusted to 9 by gradual addition of 2 mol L^{-1} of sulfuric acid. After stirring the resulted solution for 4 h, the gel obtained was filtered, washed thoroughly with demineralized water, dried at 50°C for 12 h and calcined at 540°C for 6 h.

2.3. Preparation of the ZnHCF-MCM-41

The mesoporous MCM-41 (1 g) was impregnated with 10 mL solution of $Zn(NO_3)_2$ (0.5 mol L^{-1}) for 3 h. The supernate was decanted and 5 mL solution of $K_4[Fe(CN)_6]$ (0.5 mol L^{-1}) was added dropwise under agitation at room temperature. The obtained slurries were aged at 25°C for 24 h, then washed with deionized water, filtered using a Buchner funnel with suction, followed by being dried in the oven at 50°C for 12 h.

2.4. Adsorbent characterization

A Philips X'pert powder diffractometer system with Cu-Kα (λ = 1.541 Å) radiation was used for X-ray studies. XRD analysis was performed from 1.5° to 100.0° (2θ) at a scan rate of 0.02° (2θ) s^{-1}. Nitrogen adsorption studies were made with a Quantachrome NOVA 2200e instrument. The surface morphology and chemical components of the adsorbent was characterized by scanning electron microscope (SEM) Philips XL-30 associated with energy dispersive spectroscopy. Infrared absorption spectra Fourier transform infrared spectroscopy (FTIR) were recorded with Bruker FTIR spectrophotometer model Vector-22.

2.5. Procedure for sorption studies

The adsorption studies of the cesium ion on the ZnHCF-MCM-41 adsorbent were carried out using batch method [11,12]. In this procedure, 20 mg of adsorbent was dispersed in 20 mL solution of 2×10^{-3} mol L^{-1} cesium ion. The mixture was shaken (~150 rpm) for a preselected period of time using a water shaker bath. Then, it was filtered and the amount of the cesium ion was measured using a flame atomic absorption spectrometer. The percent removal (R, %), the sorption capacity (q, mg g^{-1}), and the distribution coefficient (k_d, mL g^{-1}) were calculated using the eqs. (1), (2), and (3), respectively.

$$R = \frac{(C_i - C_f)}{C_i} \times 100 \quad (1)$$

$$q = (C_i - C_f) \times \frac{V}{m} \quad (2)$$

$$k_d = \frac{(C_i - C_f)}{C_f} \times \frac{V}{m} \quad (3)$$

where C_i and C_f, are the initial and final concentrations (mg L^{-1}) of cesium, V is the volume of the initial solution (mL), and m is the mass of the adsorbent (g).

3. Results and discussion

3.1. Characterization of the ZnHCF-MCM-41

Fig. 1(a) and (b) represent the low angle and high angle XRD patterns of the prepared ZnHCF-MCM-4 sample, respectively. Fig. 1(a) shows a strong peak at 2θ smaller than 3° along with some small peaks similar to XRD pattern of the mesoporous MCM-41 [9,10] that confirms the presence of MCM-41 in the prepared ZnHCF-MCM-41 sample. Fig. 1(b) shows the main diffraction peaks of the ZnHCF incorporated onto MCM-41. The ZnHCF loaded onto MCM-41 was identified by comparing the powder XRD pattern with those reported previously [13].

The nitrogen adsorption–desorption isotherms and pore size distribution curves of the MCM-41 and ZnHCF-MCM-41 are given in Fig. 2(a) and (b). The nitrogen adsorption–desorption isotherm of the ZnHCF-MCM-41 similar to nitrogen adsorption–desorption isotherm of the mesoporous MCM-41

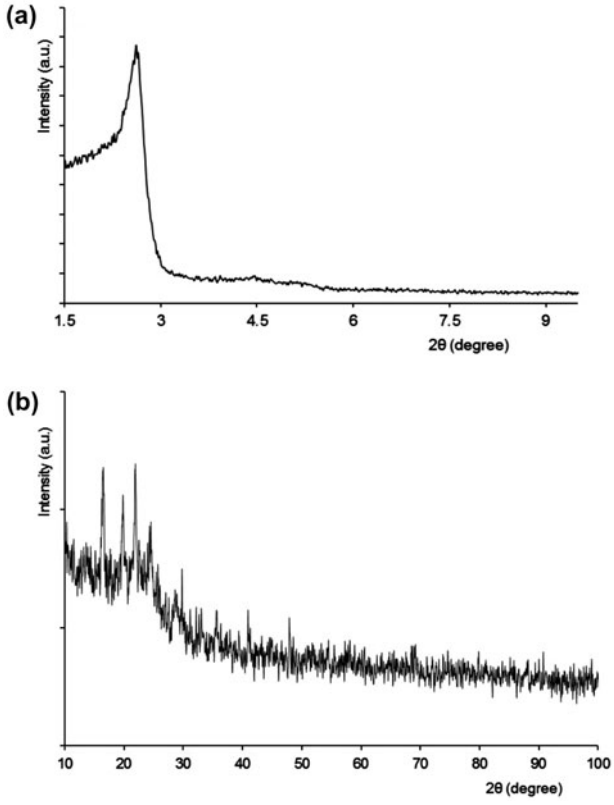

Fig. 1. Low angle (a) and high angle (b) XRD patterns of the prepared ZnHCF-MCM-41 sample.

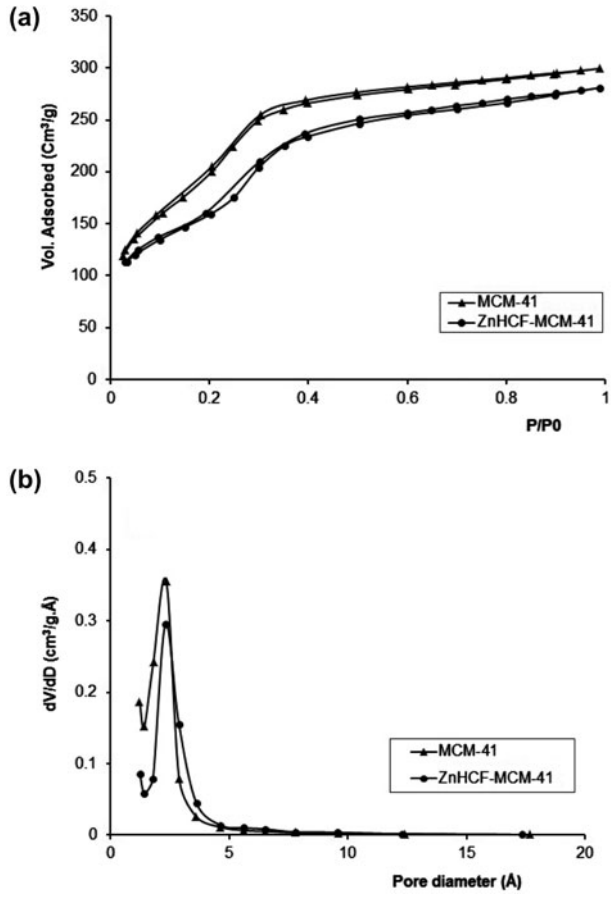

Fig. 2. Nitrogen adsorption/desorption isotherms (a) and pore size distribution curves (b) of the MCM-41 and ZnHCF-MCM-41 samples.

showed a typical adsorption profile of type IV, which consisted of a step condensation behavior due to the formation of mesopores in the MCM-41 and the presence of mesoporous MCM-41 in the ZnHCF-MCM-41 [14–16].

Table 1, shows the specific surface area, pore volume, and pore size of the MCM-41 and ZnHCF-MCM-41 samples. The BET surface area of the ZnHCF-MCM-41 sample was 585.0 $m^2 g^{-1}$, which is less than the surface area of the MCM-41 (771.4 $m^2 g^{-1}$). This may be due to the blocking of some pores mesoporous MCM-41 by entering of ZnHCF particles.

Table 1
Physical properties of the MCM-41 and ZnHCF-MCM-41

Sample	Pore volume (cc g^{-1})	BET surface area ($m^2 g^{-1}$)	Average pore diameter (nm)
MCM-41	0.46	771.4	2.34
ZnHCF-MCM-41	0.43	585.0	2.31

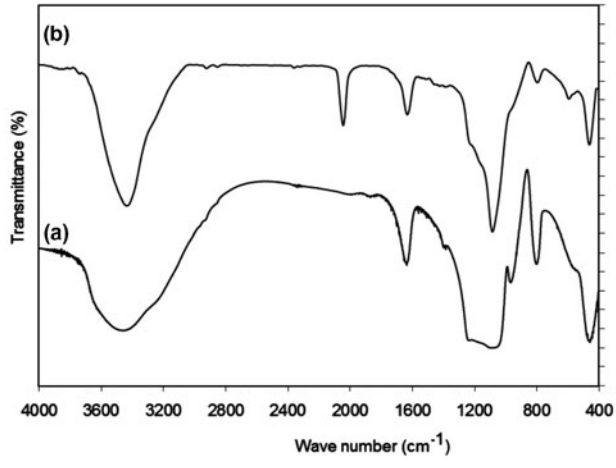

Fig. 3. FT-IR spectra of (a) MCM-41 and (b) ZnHCF-MCM-41.

Infrared spectroscopy was used to check the cyano group in ZnHCF loaded on the mesoporous MCM-41. The FTIR spectra of MCM-41 and ZnHCF-MCM-41 are shown in Fig. 3. The plot of the ZnHCF-MCM-41 is similar to that of MCM-41, except the sharp and strange peak at 2098 cm^{-1} corresponding to the C≡N stretching vibration [17] which offers the evidence that ZnHCF is loaded on the MCM-41, after carefully isolated from the mentioned preparation system.

Fig. 4(a) and (b) show SEM image and EDX spectrum pattern of the ZnHCF-MCM-41. The fine ZnHCF crystals are seen to be precipitated onto the internal–external surfaces of the framework of the MCM-41. The EDX spectrum pattern from Fig. 4(b) shows the strong silicon peak from the mesoporous silicate MCM-41 support. Besides the K, Zn, and Fe peaks from the ZnHCF crystals loaded on the surface of MCM-41 are also observed, which offers the evidence that ZnHCF is loaded on the MCM-41.

3.2. Adsorption test

3.2.1. Effect of the solution pH

The pH solution is a crucial factor in metal sorption. In this study, the effect of pH on cesium adsorption onto ZnHCF-MCM-41 was studied in the range 1.0–9.0. Fig. 5 shows the dependence of the

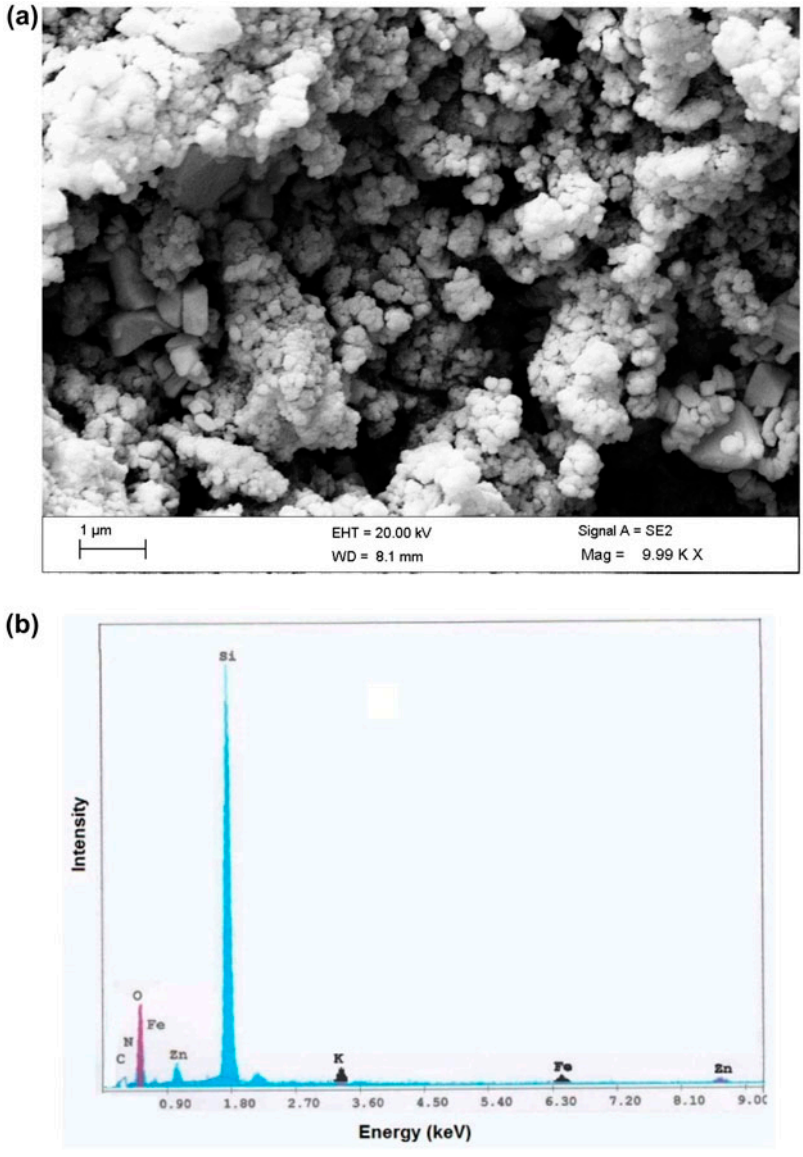

Fig. 4. SEM image of ZnHCF-MCM-41 (a); EDX area analysis of ZnHCF-MCM-41 (b).

adsorption capacity of the ZnHCF-MCM-41 on initial pH of cesium solution. The ion exchange behavior of sodium ZnHCF (II) ($Na_2Zn_3[(Fe(CN)_6]_2$) has been studied by Kawamura et al. [18]. They were reported that cesium ions were exchanged with sodium ions stoichiometrically and the involvement of cesium–zinc or cesium–iron exchange was not observed. This suggests that sodium or potassium ions are only exchangeable species in the compound. According to reports of Vlasselaer et al. [19], cesium adsorption mechanism on to potassium ZnHCF is also ion exchange of cesium with potassium. Cesium sorption onto ZnHCF-MCM-41 was low in pHs less than 4.0, that shows a significant competition of H^+ ions with cesium ions for the same site binding of adsorbent, since that ion exchange is the main mechanism of cesium adsorption. Also, by influence of low pH solution, it could come to destruction of adsorbent, which would lead also to the decrease of sorption capacity of the adsorbent [20]. According to the results of this initial experiment, further adsorption investigations were performed at pH value of 4.0 as optimal value.

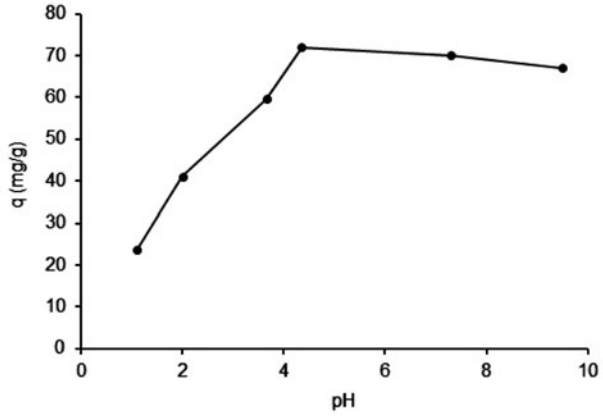

Fig. 5. Effect of pH on cesium adsorption onto ZnHCF-MCM-41. Conditions: initial concentration of cesium: 2×10^{-3} mol L^{-1}, agitation time 5 h and temperature of 25°C.

3.2.2. Effect of contact time (kinetic analysis)

In order to investigate the controlling mechanism of adsorption processes such as mass transfer and chemical reaction, the pseudo-first-order and pseudo-second-order equations are applied to model the kinetics of cesium adsorption onto ZnHCF-MCM-41. The pseudo-first-order kinetic and the pseudo-second-order kinetics are expressed by Eqs. (4) and (5), respectively.

$$\log(q_e - q_t) = \log q_e - \frac{k_1}{2.303}t \tag{4}$$

$$\frac{t}{q_t} = \frac{1}{k_2 q_e^2} + \frac{t}{q_e} \tag{5}$$

where q_e and q_t are the adsorbed metal in mg g^{-1} on the adsorbent at equilibrium and time t, respectively, k_1 is the constant of first-order adsorption in min^{-1} and k_2 is the rate constant of second-order adsorption in g mg^{-1} min^{-1} [11,12].

As seen in Fig. 6(a), the removal of cesium ions from aqueous solution by ZnHCF-MCM-41 as a function of contact time showed that 5 h was sufficient for the adsorption equilibrium to be achieved. The rate of metal ions adsorption, one of the important characteristics that define the efficiency of sorption, was evaluated by fitting the experimental data to the pseudo-first-order and pseudo-second-order kinetics. The parameters of the kinetic models and the regression correlation coefficients (R^2) are listed in Table 2. From the R^2 and the predicted q_e it was found that the pseudo-second-order kinetic model fitted the kinetic data of the adsorbent ZnHCF-MCM-41 better than that of the pseudo-first-order. The pseudo-first-order and pseudo-second-order linear plots are shown in Fig. 6(b) and (c), respectively. The confirmation of pseudo-second-order kinetics indicates that the concentrations of both adsorbate (cesium ions) and adsorbent (ZnHCF-MCM-41) are involved in the rate determining step of the adsorption process [21].

Table 2
Kinetic adsorption parameters obtained using pseudo-first-order and pseudo-second-order models (initial concentration of cesium ion 2×10^{-3} mol L^{-1})

Pseudo-first-order			Pseudo-second-order		
k_1 (min^{-1})	q_e (mg g^{-1})	R^2	k_2 (g mg^{-1} min^{-1})	q_e (mg g^{-1})	R^2
0.0007	20.12	0.937	10288.5	74.63	0.997

3.2.3. Effect of temperature (thermodynamic analysis)

The adsorption experiment was carried out at different temperatures (25, 45 and 65°C) to evaluate thermodynamic criteria by calculating the Gibbs free energy (ΔG°) by the following equation [11,12]:

$$\ln k_d = \frac{\Delta S^{\circ}}{R} - \frac{\Delta H^{\circ}}{RT} \quad (6)$$

where the ΔH° (change in enthalpy in J mol^{-1}) and ΔS° (change in entropy in J mol^{-1} K^{-1}) are obtained from slope and intercept of ln k_d vs. $1/T$ plots. T is the temperature in K and R is the universal gas constant (8.314 J mol^{-1} K^{-1}).

The ΔG° is the change in Gibbs free energy in J mol^{-1}, calculated according to the following equation [11,12]:

$$\Delta G^{\circ} = \Delta H^{\circ} - T\Delta S^{\circ} \quad (7)$$

The effect of temperature on the adsorption of cesium ions onto ZnHCF-MCM-41 is shown by the linear plot of ln k_d vs. $1/T$ in Fig. 7 and the relative parameters and correlation coefficients calculated from Eqs. (6) and (7) are listed in Table 3. The positive values of ΔH° and the increasing value of k_d with increasing temperature indicate that the sorption of cesium ions onto the ZnHCF-MCM-41 is an endothermic process, and thus better adsorption properties, at higher temperature, were obtained. Expect notification endothermicity of adsorption processes, the positive value of ΔS° indicates feasible adsorption. It is noticeable that the ΔG° values decrease with increasing temperature, indicating higher spontaneity at higher temperatures. It was found that free energy change for physisorption is generally ranges between −20 and 0 kJ mol^{-1}, the physisorption together with chemisorption within −20 to −80 kJ mol^{-1}, and pure chemisorption in the range of −80 to −400 kJ mol^{-1} [22]. The calculated ΔG° values suggest that the sorption processes of cesium on the ZnHCF-MCM-41 could be considered as physisorption process.

3.2.4. Effect of initial metal ion concentration (isotherm analysis)

In order to determine the relationship between the amount of cesium ions adsorbed on the adsorbent surface and the concentration of remaining metal ions in the aqueous phase, the adsorption isotherm studies were performed. Among various binding models, the

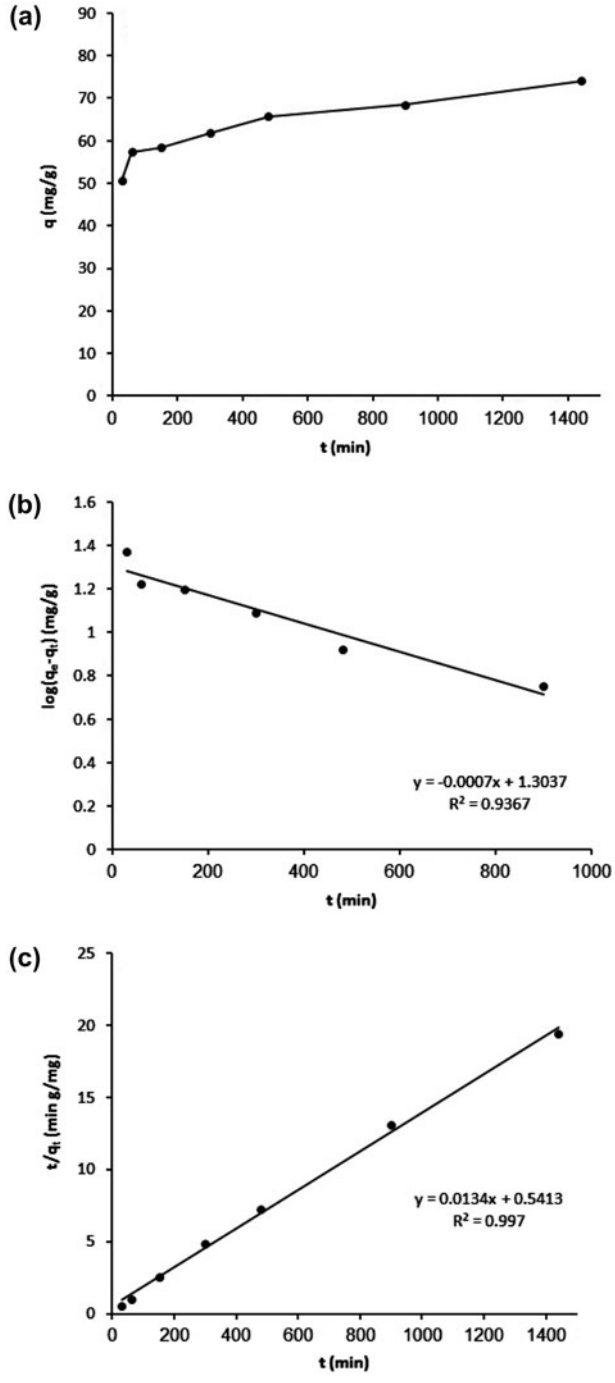

Fig. 6. Adsorption kinetics of cesium onto ZnHCF-MCM-41(a), pseudo-first-order and pseudo-second-order linear plot ((b) and (c)). Conditions: initial concentration of cesium: 2×10^{-3} mol L^{-1}, initial pH value 8.0 and temperature of 25°C.

Langmuir and Freundlich isotherms have been frequently employed to describe the experimental data of adsorption isotherms. The Langmuir and Freundlich

Table 3
Thermodynamic parameters of Cs adsorption on ZnHCF-MCM-41 at different temperatures in Kelvin (initial concentration of cesium ion 2×10^{-3} mol L^{-1})

		ΔG° (kJ mol^{-1})			
ΔH° (kJ mol^{-1})	ΔS° (J^{-1} mol^{-1} K^{-1})	298	318	338	R^2
7.64	0.08	−16.36	−17.97	−19.58	0.989

adsorption isotherms are mathematically expressed in Eqs. (8) and (9) respectively [12,13].

$$\frac{1}{q_e} = \frac{1}{q_{\max}} + \frac{1}{k_1 q_{\max} C_e} \tag{8}$$

$$\ln q_e = \ln k_f + m \ln C_e \tag{9}$$

where q_e (mg g^{-1}) is the amount of analyte bound to the adsorbent, C_e (mg L^{-1}) is the equilibrium concentration of the adsorbate in solution, $q_{\max}$ is the maximum adsorption capacity (mg g^{-1}), and K_f, K_l, and m are constants for a given adsorbate and adsorbent at a particular temperature.

Fig. 8(a) shows the experimental, Langmuir and Freundlich model isotherms. Fig. 8(b) and (c) also shows linear Langmuir and Freundlich plots. The Langmuir isotherm model fitted the experiment data better than Freundlich isotherm model. The Langmuir model is used for homogeneous surfaces with identical binding sites. The values of the fitting parameters and correlation coefficient are shown in Table 4. As seen, the calculated maximum adsorption capacity ($q_{\max}$) was 103.09 mg g^{-1}.

A comparison of ZnHCF-MCM-41 adsorbent performance for cesium removal from aqueous solutions

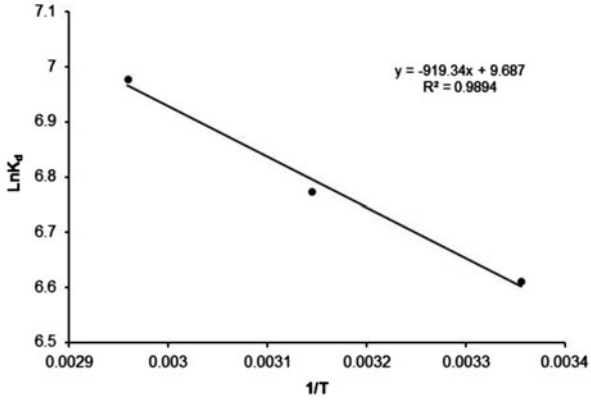

Fig. 7. Plots of ln k_d vs. $1/T$ for cesium adsorption on ZnHCF-MCM-41. Conditions: initial concentration of cesium: 2×10^{-3} mol L^{-1}, initial pH value 8.0, agitation time 5 h.

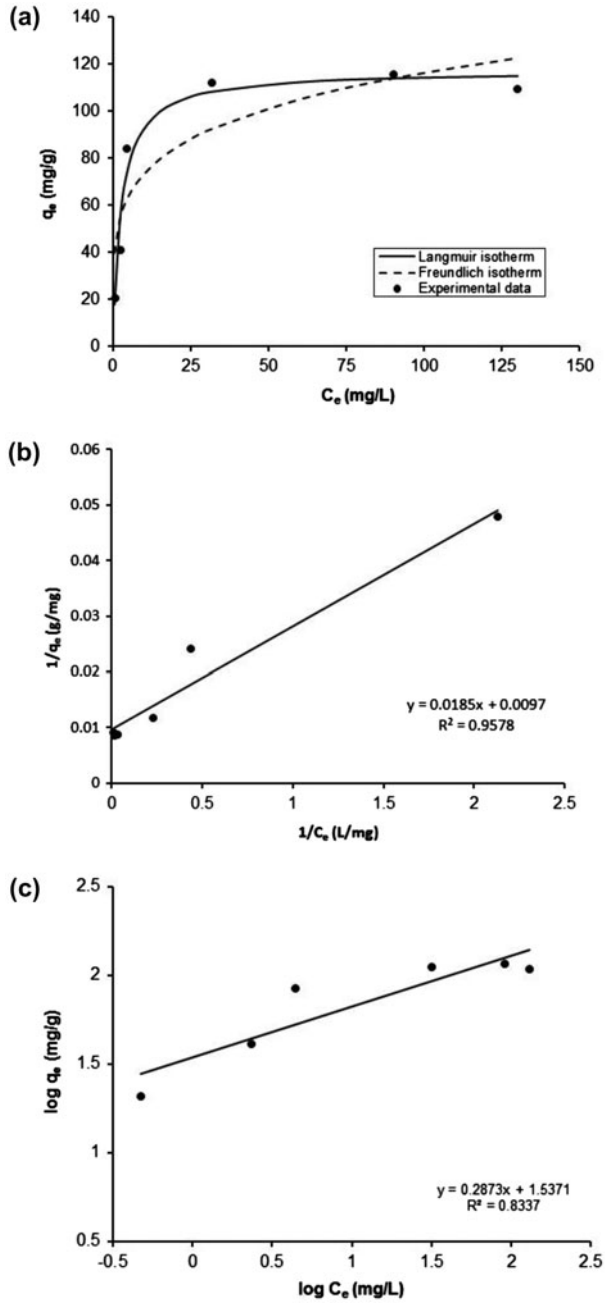

Fig. 8. Adsorption isotherms of ZnHCF-MCM-41 for cesium adsorption (a), Linearized Langmuir and Freundlich plot ((b) and (c)). Conditions: initial pH value 8.0, agitation time 5 h and temperature of 25°C.

Table 4
Langmuir and Freundlich isotherm model fitting parameters for cesium

Models	Fitting parameters		
Langmuir	R^2	K_l (L mg^{-1})	q_{max} (mg g^{-1})
	0.958	0.52	103.09
Freundlich	R^2	K_f (mg g^{-1} mg^{-m} L^m)	m
	0.834	34.44	0.29

Table 5
Comparison of cesium adsorption by ZnHCF-MCM-41 in this study with other adsorbents from literatures

Adsorbent	q_{max} (mg g^{-1})	Ref.
Composite sorbent[a]	19.94	[1]
Indion-810 resin[b]	47.85	[23]
Silica gel[c]	54.49	[24]
Activated carbon[d]	63.80	[7]
ZnHCF-MCM-41	103.9	This work

[a]Copper hexacyanoferrate/polymer/silica composites.
[b]Modified with copperhexacyanoferrate.
[c]Modified with potassium nickel hexacyanoferrate.
[d]Modified with potassium copper hexacyanoferrate.

with different adsorbents reported in literature [1,7,23,24] is given Table 5. Comparison of q_{max} values showed that the adsorption capacity of the ZnHCF-MCM-41 prepared in our work was higher than the previously reported values. The high adsorption capacity of the ZnHCF-MCM-41 is probably due to high selectivity of ZnHCF loaded onto mesoporous MCM-41 and also high surface area of ZnHCF-MCM-41 adsorbent than other amorphous adsorbents.

4. Conclusion

A new adsorbent (ZnHCF-MCM-41) was synthesized by loading of ZnHCF on mesoporous MCM-41 and showed high efficiency for the removal of cesium ions from aqueous solutions. The Langmuir isotherm fitted the equilibrium data better than the Freundlich isotherm that demonstrated homogeneous surfaces with identical binding sites for ZnHCF-MCM-41. The kinetics of cesium adsorption onto ZnHCF-MCM-41 reveals that cesium ions are adsorbed satisfactorily according to the pseudo-second-order equation and the concentrations of both sorbate and adsorbent are involved in the rate-determining step of the adsorption process. The value of thermodynamic parameters confirmed the feasibility and spontaneity, as well as the endothermic nature of the adsorption process of the cesium ions onto ZnHCF-MCM-41, as the change in enthalpy was found to be positive.

References

[1] S. Milonji, I. Bispo, M. Fedoroff, C. Loos-Neskovic, C. Vidal-Madjar, Sorption of cesium on copper hexacyanoferrate/polymer/silica composites in batch and dynamic conditions, J. Radioanal. Nucl. Chem. 252 (2002) 497–501.
[2] C.Y. Chang, L.K. Chau, W.P. Hu, Nickel hexacyanoferrate multilayers on functionalized mesoporous silica supports for selective sorption and sensing of cesium, Microporous Mesoporous Mater. 109 (2008) 505–512.
[3] H.H. Someda, A.A. ElZahhar, M.K. Shehata, H.A. El-Naggar, Supporting of some ferrocyanides on polyacrylonitrile (PAN) binding polymer and their application for cesium treatment, Sep. Purif. Technol. 29 (2002) 53–61.
[4] H. Mimura, M. Kimura, K. Akiba, Selective removal of cesium from sodium nitrate solutions by potassium nickel hexacyanoferrate-loaded chabazites, Sep. Sci. Technol. 34 (1999) 17–28.
[5] H. Kazemian, H. Zakeri, M.S. Rabbani, Cs and Sr removal from solution using potassium nickel hexacyanoferrate impregnated zeolites, J. Radioanal. Nucl. Chem. 268 (2006) 231–236.
[6] C.T. Huang, G. Wu, Improvement of Cs leaching resistance of solidified radwastes with copper ferrocyanide (CFC)-vermiculite, Waste Manage. 19 (1999) 263–268.
[7] L. Wang, M. Feng, C. Liu, Y. Zhao, S. Li, H. Wang, L. Yan, G. Tian, S. Li, Supporting of potassium copper hexacyanoferrate on porous activated carbon substrate for cesium separation, Sep. Sci. Technol. 44 (2009) 4023–4035.
[8] Y.H. Lin, G.E. Fryxell, H. Wu, Selective sorption of cesium using self-assembled monolayers on mesoporous supports, Environ. Sci. Technol. 35 (2001) 3962–3966.
[9] C.T. Kresge, M.E. Leonowicz, W.J. Roth, J.C. Vartuli, J.S. Beck, Ordered mesoporous molecular sieves synthesized by a liquid-crystal template mechanism, Nature 359 (1992) 710–712.
[10] J.S. Beck, J.C. Vartuli, W.J. Roth, M.E. Leonowicz, C.T. Kresge, K.D. Schmitt, C.T.W. Chu, D.H. Olson, E.W. Sheppard, S.B. McCullen, J.B. Higgins, J.L. Schlenker, A new family of mesoporous molecular sieves prepared with liquid crystal templates, J. Am. Chem. Soc. 114 (1992) 10834–10843.
[11] H. Tavakoli, H. Sepehrian, R. Cheraghali, Encapsulation of nanoporous MCM-41 in biopolymeric matrix of calcium alginate and its use as effective adsorbent for lead ions: Equilibrium, kinetic and thermodynamic studies, J. Taiwan Inst. Chem. Eng. 44 (2013) 343–348.
[12] R. Chreaghali, H. Tavakoli, H. Sepehrian, Preparation, characterization and lead sorption performance of Alginate-SBA-15 composite as a novel adsorbent, Scientia Iranica 20 (2013) 1028–1034.
[13] C.A. Chugh, D. Bharti, Antifungal potential of transition metal hexacyanoferrates against fungal diseases of mushroom, Open J. Syn. Theory Appl. 1 (2012) 23–30.
[14] F. Rouquerol, I. Rouquerol, K. Sing, Adsorption by Powder and Porous Solids, Academic Press, London, 1990.

[15] S.J. Gregg, K.S.W. Sing, Adsorption Surface Area and Porosity, Academic Press, London, 1982.
[16] J.B. Condon, Surface Area and Porosity Determination by Physisosorptio, Elsevier, London, 2006.
[17] K. Nakamoto, Infrared and Raman Spectra of Inorganic and Coordination Compounds, 4th ed., Wiley, New York, NY, 1986.
[18] S. Kawamura, H. Kuraku, K. Kurotaki, The composition and ion-exchange behavior of zinc hexacyanoferrate(II) analogues, Anal. Chim. Acta 49 (1970) 317–322.
[19] S. Vlasselaer, W. D'Olieslager, M. D'Hont, Caesium ion exchange equilibrium on potassium-zinc-hexacyanoferrate(II) $K_2Zn_3(Fe(CN)_6)_2$, J. Inorg. Nucl. Chem. 38 (1976) 327–330.
[20] Ľ. Vrtoch, M. Pipíška, M. Horník, J. Augustín, J. Lesný, Sorption of cesium from water solutions on potassium nickel hexacyanoferrate-modified *Agaricus bisporus* mushroom biomass, J. Radioanal. Nucl. Chem. 287 (2011) 853–862.
[21] C.C. Liu, M. Kuang-Wang, Y.S. Li, Removal of nickel from aqueous solution using wine processing waste sludge, Ind. Eng. Chem. Res. 44 (2005) 1438–1445.
[22] M.M. Rao, G.P.C. Rao, K. Seshaiah, N.V. Choudary, M.C. Wang, Activated carbon from Ceiba pentandra hulls, an agricultural waste, as an adsorbent in the removal of lead and zinc from aqueous solutions, Waste Manage. 28 (2008) 849–858.
[23] I.J. Singh, B.M. Misra, Studies on sorption of radiocesium on copper-hexacyanoferrate-loaded resins, Sep. Sci. Technol. 31 (1996) 1695–1705.
[24] P. Rajec, J. Orechovská, I. Novák, NIFSIL: A new composite sorbent for cesium, J. Radioanal. Nucl. Chem. 245 (2000) 317–321.